

Lagrangian Velocity Fluctuations in Fully Developed Turbulence: Scaling, Intermittency, and Dynamics

N. Mordant,¹ J. Delour,¹ E. L eveque,¹ O. Michel,^{1,2} A. Arn edo,¹ and J.-F. Pinton¹

Received ■■; accepted February 26, 2003

New aspects of turbulence are uncovered if one considers the flow motion from the perspective of a fluid particle (known as the Lagrangian approach) rather than in terms of a velocity field (the Eulerian viewpoint). Using a new experimental technique, based on the scattering of ultrasound, we have obtained a direct measurement of particle velocities, resolved at all scales, in a fully turbulent flow. We find that the Lagrangian velocity autocorrelation function and the Lagrangian time spectrum are in agreement with the Kolmogorov K41 phenomenology. Intermittency corrections are observed and we give a measurement of the Lagrangian structure function exponents. They are more intermittent than the corresponding Eulerian exponents. We also propose a novel analysis of intermittency in turbulence: our measurement enables us to study it from a *dynamical* point of view. We thus analyze the Lagrangian velocity fluctuations in the framework of random walks. We find experimentally that the elementary steps in the “walk” have random uncorrelated directions but a magnitude that displays extremely long-range correlations in time. Theoretically, we study a Langevin equation that incorporates these features and we show that the resulting dynamics accounts for the observed one-point and two-point statistical properties of the Lagrangian velocity fluctuations. Our approach connects the intermittent statistical nature of turbulence to the dynamics of the flow.

KEY WORDS: Lagrangian; turbulence; scaling; intermittency.

1. INTRODUCTION

Traditional experimental studies of velocity fluctuations in homogeneous, isotropic, three-dimensional turbulence rely on velocimetry measurements

¹Laboratoire de Physique,  cole Normale Sup rieure de Lyon, 46 all e d’Italie, F-69007 Lyon, France; e-mail: pinton@ens-lyon.fr

²Laboratoire d’Astrophysique, Universit  de Nice, Parc Valrose, F-06108 Nice, France.

at a fixed point in space. A local velocity probe yields time traces of the velocity fluctuations which are then related to spatial velocity profiles using the Taylor hypothesis. In this case, the flow is analyzed in terms of the Eulerian velocity field $\vec{u}(x, t)$. Several features are now firmly established about the Eulerian velocity field:⁽¹⁾ the Kolmogorov $k^{-5/3}$ spectrum, the associate “4/5th” law, and the presence of intermittency corrections. In the Lagrangian framework, the flow is described by the motion of individual fluid particles; the velocity $\vec{v}(\vec{a}, t)$ as a function of time of a fluid particle located at position \vec{a} at initial time. It is a natural framework for mixing and transport problems. It has also been shown theoretically in the passive scalar problem that intermittency is strongly connected to the particular properties of Lagrangian trajectories.^(2,3) However Lagrangian measurements are challenging because they involve the tracking of particle trajectories: enough time resolution, both at small and large scales, is required to describe the turbulent fluctuations.

We have developed a new experimental method, based on sonar techniques,⁽⁴⁾ in order to study in a laboratory experiment the velocity of tracer particles across the inertial range of time scales. We derive from our measurements the Lagrangian velocity auto-correlation function and time spectrum which are found to be in very good agreement with the Kolmogorov K41 picture of turbulence. We also compute higher order statistics and firmly establish the existence of intermittency in Lagrangian coordinates. However, we take a further step. In the Eulerian framework, intermittency is attributed to the inhomogeneity in space of the turbulent activity and often analyzed in terms of ad hoc multiplicative cascade models. Although very successful at describing the data, these models have failed to connect intermittency with the dynamical equations that govern the motion of the fluid. Since our measurements give access to the individual motion of fluid particles, we study intermittency from a dynamical point of view. We show that the observed anomalous scaling in the Lagrangian velocity increments traces back to the existence of long-time correlations in the particle accelerations, i.e., the hydrodynamic forces that drive the particle motion. We believe that these long-time correlations are of fundamental importance both for the understanding of turbulence and for stochastic models that are used to describe particle dynamics in turbulent flows.

2. EXPERIMENTAL SETUP

In order to study the dynamics of Lagrangian tracers, we need to resolve their velocity fluctuations across a wide range of scales. To this end, we use a confined flow with no mean advection, so that fluid particles

remain for long times inside a given measurement volume. A water flow of the von Kármán swirling type⁽⁵⁻⁸⁾ is generated inside a cylinder by counter-rotation at a variable frequency $1/2$ of two discs with radius $R = 9.5$ cm, fitted with eight blades of height 0.5 cm and set 18 cm apart—Fig. 1(a). The large scale flow is axisymmetric and the fluctuations in its center approximate the conditions of local homogeneous and isotropic turbulence. The Taylor microscale λ_T in the flow varies from 600 to 900 microns, larger than the diameter (250 μm) of the neutrally buoyant tracer particle (density of 1.06)—see Table I. However, the particle size is larger than the Kolmogorov dissipative scale η , so that a frequency cut-off is expected in the way the solid particles follow the fluid motion. We will see that the particles act as Lagrangian tracers for times longer than 1 ms.

The tracking of the tracer particles is achieved using a new acoustic technique, based on the principle of a “continuous Doppler sonar.” The

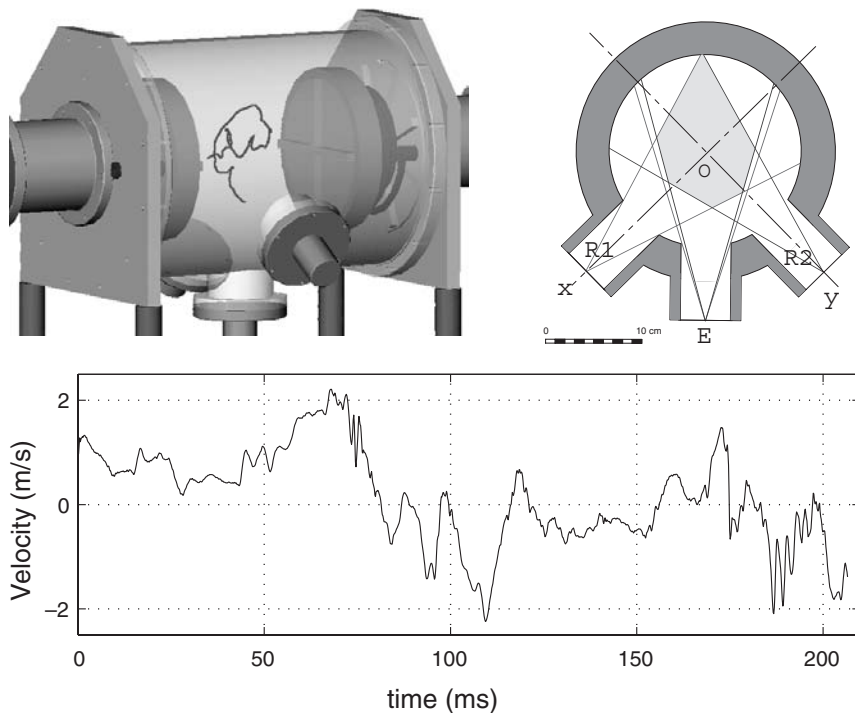


Fig. 1. (a) Left: set-up and example of a particle trajectory, 206 ms ($= 9.2T_L$) long, where T_L is the integral time scale. Right: acoustics; the emitter is located at (E) and two arrays of receivers at (x) and (y) detect the sound scattered by the particle when it moves inside the shaded volume. (b) Example of detected velocity variations (one component shown).

Table 1. Main Characteristics of the Turbulence Produced in the von Kármán Swirling Flow^a

Ω [Hz]	ϵ [W/kg]	u_{rms} [m/s]	λ_T [μm]	T_L [ms]	τ_η [ms]
4	8	0.48	650	46.7	0.35
7.2	25	0.98	880	22.4	0.20
11	72	1.58	920	14.7	0.12

^a Ω is the frequency of counter-rotation of the driving discs; ϵ is the flow power consumption per unite mass; u_{rms} is the standard deviation of the velocity fluctuations in the center of the flow; λ_T is the Taylore microscale; T_L the integral time of the Lagrangian motion (measured from the autocorrelation of the Lagrangian velocity), and τ_η is the Kolmogorov dissipative time scale.

flow volume is continuously insonified with a monochromatic ultrasound, which is then scattered by the tracer particle.^(4,9) This scattered sound is detected by two transducer arrays, which yield a measurement of both the particle position, by direct triangulation, and of its velocity, from the Doppler shift. Indeed, for an incoming sound with frequency f_0 , the scattered sound at the receiver has frequency $f(t) = f_0 + \mathbf{k} \cdot \mathbf{v}(t)$, where $\mathbf{v}(t)$ is the velocity of the tracer particle and \mathbf{k} is the scattering wave vector. The flow is insonified at 2.5 MHz, with the transducers located at the flow wall. The receiver arrays are placed at 45 degrees on each side of the emission direction. The measurement region is the intersection of the emission and detection cones, as shown in Fig. 1(b); the volume defined in this manner is neither axisymmetric nor isotropic and this introduces a bias that must be taken into account in the averaging process.⁽¹⁰⁾ The scattered acoustic signal is recorded on an array of transducers and the frequency modulation is extracted numerically, using a high-resolution parametric method.^(4,11,12) The particles are tracked as long as they stay confined insided the measurement volume, i.e., between one and ten T_L , the Lagrangian integral time scale (computed from the Lagrangian velocity autocorrelation function). Figure 1(c) gives an example of the time variation of one component of a particle's velocity. 4000 such events are analyzed, i.e., 1.9×10^6 data points sampled at 6.5 kHz.

3. "K41" SECOND ORDER QUANTITIES

Let us first consider the Lagrangian velocity auto-correlation function:

$$R^L(\tau) = \frac{\langle v(t) v(t+\tau) \rangle_t}{\langle v^2 \rangle}. \quad (1)$$

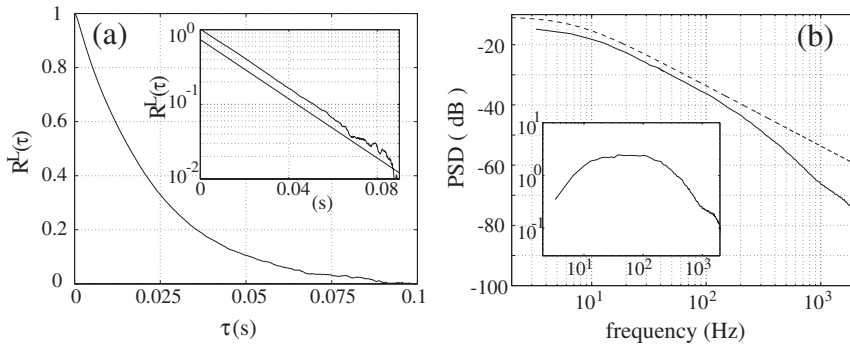


Fig. 2. Autocorrelation function and spectrum of the Lagrangian velocity at $R_\lambda = 740$. (a) Velocity autocorrelation function. A best exponential fit is $\rho_v^L(\tau) = 1.03e^{-45.7\tau}$. It is shown, slightly shifted for clarity, as the linear curve in the inset. (b) Corresponding power spectrum; the upper curve dashed is the Lorentzian function calculated from the exponential fit of the auto-correlation function (shifted for clarity). The inset shows the power spectrum compensated by an ω^{-2} scaling: the plateau corresponds to the region of Kolmogorov scaling.

We observe—Fig. 2a—that it has a slow decrease which can be modeled by an exponential function $\rho_v^L(\tau) \sim e^{-\tau/T_L}$. This expression defines an integral Lagrangian time scale $T_L = 22$ ms. For comparison, the period of rotation of the discs is 140 ms and the sweeping period of the blades is 17 ms. The measured Lagrangian time scale thus appears as a time characteristic of the energy injection. The exponential reproduces extremely well the variation of the auto-correlation function, from about $5\tau_\eta$ at small scales to $4T_L$ —see inset of Fig. 2a. These limits coincide with the upper and lower resolutions of the technique, so that we observe an exponential decay over the entire range of our measurement. Note that, as the variance of the acceleration must be finite⁽¹³⁾ there has to be some lower cut-off to this behavior, at times of order τ_η . These observations extend and confirm previous numerical and experimental studies at moderate Reynolds numbers.^(14–16) The exponential decay of the Lagrangian velocity auto-correlation is a key feature of stochastic models of dispersion since it appears as a linear drift term in a Langevin model of particle dynamics.^(17,18)

We then turn to the Lagrangian spectrum, i.e., the power spectrum in time of velocity fluctuations of the tracer particle. From the exponential fit shown in Fig. 2b, and by computing the Fourier transform of the exponential decay of the auto-correlation function, one gets:

$$E_{\text{fit}}^L(\omega) = \frac{u_{\text{rms}}^2 T_L}{1 + (T_L \omega)^2}. \quad (2)$$

We observe a clear range of power law scaling $E^L(\omega) \propto \omega^{-2}$ —see the compensated plot inset of Fig. 2b. This is in agreement with a Kolmogorov K41 picture in which the spectral density at a frequency ω is a dimensional function of ω and ϵ : $E^L(\omega) \propto \epsilon \omega^{-2}$. To our knowledge, this is the first time that this scaling is directly observed at high Reynolds number and in a laboratory experiment, although it has been reported in oceanic studies⁽¹⁹⁾ and in lower Reynolds number direct numerical simulations.⁽²⁰⁾ Departure from the Kolmogorov behavior is observed at low frequencies in agreement with the exponential decay of the auto-correlation. At high frequencies, the spectrum deviates from the Lorentzian form due to the particle response (inertia). A typical response time for the particle is of the order of d/u_{rms} , where d is its diameter; for the 250 μm particles used here this corresponds to a frequency cut-off of about one kiloHertz, as observed in Fig. 2b.

Staying with second order statistical quantities, we now consider the second order structure function of the velocity increment

$$D_2^L(\tau) = \langle (v(t+\tau) - v(t))^2 \rangle_t = \langle (A_\tau v)^2 \rangle. \quad (3)$$

(We emphasize that the Lagrangian increments are made over time, and not in space as in the Eulerian domain). The second order structure function is related to the velocity auto-correlation function by $D_2^L(\tau) = 2u_{\text{rms}}^2(1 - R^L(\tau))$: at small times one observes the trivial scaling $D_2^L(\tau) \propto \tau^2$ and at large times $D_2^L(\tau)$ saturates at $2u_{\text{rms}}^2$ (as $v(t)$ and $v(t+\tau)$ become uncorrelated). In between these two limits, one expects an inertial range of scales with a Kolmogorov-like scaling

$$D_2^L(\tau) = C_0 \epsilon \tau, \quad (4)$$

where C_0 is a “universal” constant. Such a behavior is consistent with dimensional analysis and with an ω^{-2} scaling range in the velocity power spectrum. Figure 3 shows $D_2^L(\tau)/\epsilon\tau$; a plateau with a constant C_0 is not observed. At $R_\lambda \sim 1000$, the function reaches a maximum at $20\tau_\eta$, for which $C_0 \sim 2.9$. This value is in agreement with the estimation $C_0 = 4 \pm 2$ in ref. 21 and in the range of values (between 3 and 7) used in stochastic models for particle dispersion.⁽²²⁾ However, in our set of measurements between $R_\lambda = 100$ and $R_\lambda = 1100$, we have observed an increase of C_0 (defined in the same way) from 2.5 to 3.5. We point out that in the absence of an equivalent of the Kármán–Howarth relationship for the Lagrangian time increments, a limit value of C_0 is not *a priori* fixed. Dimensional analysis yields $D_2^L(\tau) = C_0(\text{Re}) \epsilon \tau$ and similarity arguments give $C_0(\text{Re}) \rightarrow \text{const.}$ or $C_0(\text{Re}) \rightarrow \text{Re}^\alpha$ in the limit of infinite Reynolds numbers (in the latter case, α is a critical exponent to be determined independently).

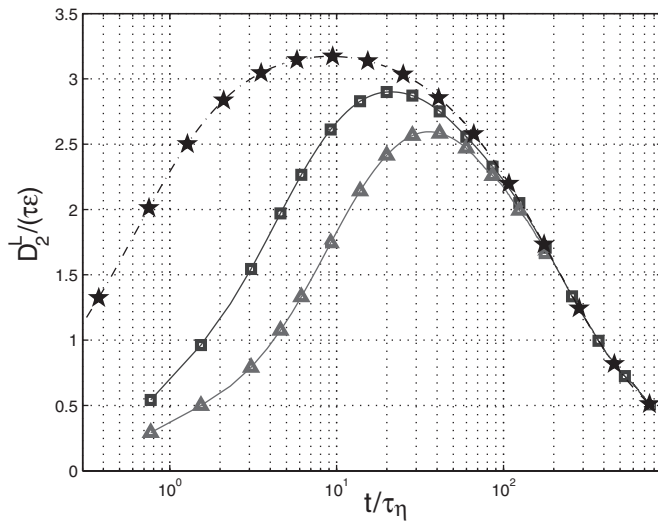


Fig. 3. Second order structure function, normalized by the Kolmogorov scaling $\epsilon\tau$, plotted for three Reynolds numbers. Triangles corresponds to $R_\lambda = 312$ and a maximum C_0 value of 2.6. Squares: $R_\lambda = 740$ and $C_0 = 2.8$. Stars: $R_\lambda = 1100$ and $C_0 = 3.2$.

4. INTERMITTENCY AND SCALING

In order to further describe the statistics of the Lagrangian velocity fluctuations, one must turn to higher order statistics of the velocity increments $\Delta_\tau v$. Their PDF Π_τ for τ covering the accessible range of time scales is shown in Fig. 4, where the variations have been normalized to unit variance in order to emphasize changes in the functional forms. A first observation is that the PDFs are symmetric about $\Delta v = 0$, in agreement with the local symmetries in this flow (there is no expected skewness in the Lagrangian velocity fluctuations). At the smallest increment, the stretched exponential shape is in agreement with measurements of the PDF of Lagrangian acceleration at identical Reynolds numbers.⁽²³⁾ In our case, the limit form of the PDF of the velocity increments is not as wide as that of the acceleration because the Kolmogorov scale is not resolved. At large time increments the PDFs become Gaussian, as in Eulerian statistics. In between these extremes, the change is continuous, as the PDFs develop stretched exponential tails as the time increments decrease.

The variation of the PDFs of velocity increments with scale is often described in terms of the scaling of structure functions:

$$D_q^L(\tau) = \langle |\Delta_\tau v|^q \rangle \sim \tau^{\zeta^L(q)}. \quad (5)$$

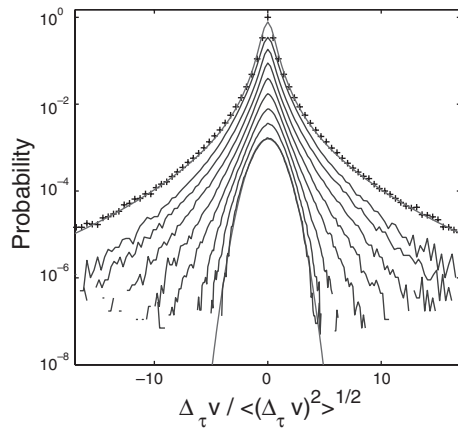


Fig. 4. PDF $\sigma_\tau \Pi_\tau$ of the normalized increment $\Delta v_\tau / \sigma_\tau$, at $R_\lambda = 740$. The curves are shifted for clarity. From top to bottom: $\tau = [0.15, 0.3, 0.6, 1.2, 2.5, 5, 10, 20, 40]$ ms. The underlying crosses in the outer curve correspond to the MRW model presented in Section 5.2, with $\lambda^2 = 0.115$.

They are plotted in Fig. 5, for orders up to the sixth (this limit being due to the number of experimental data point available, $\sim 10^6$). The extent of the inertial range is too small to observe a true scaling region in the $D_q^L(\tau)$ plots—Fig. 5(a).

We thus estimate the scaling exponents using the ESS ansatz that has become classical in the analysis of the Eulerian structure function.⁽²⁴⁾ In Lagrangian coordinates, one has to use the second order structure function

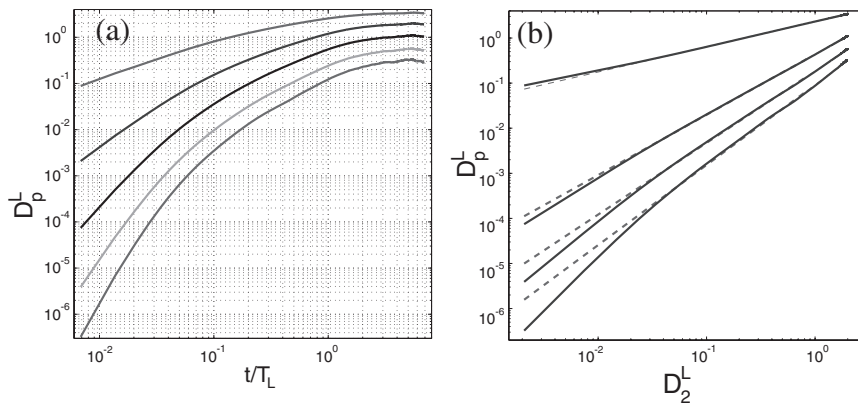


Fig. 5. Lagrangian velocity structure functions, for $R_\lambda = 740$; (a) $D_q^L(\tau)$ in logarithmic scales; (b) relative behavior of D_q^L vs. D_2^L . The dashed lines are best linear fits with slope in the inertial range $\xi^L(q) = 0.56, 1.33, 1.56, 1.73$ for $q = 1, 3, 4, 5$.

as a reference, because dimensional analysis show that it is that moment of the velocity increments which varies linearly on the energy transfer ϵ (as the third order structure function D_3^E in Eulerian coordinates). In this case one observes a relative scaling—cf. Fig. 5(b)

$$D_q^L(\tau) \propto [D_2^L(\tau)]^{\xi^L(q)}. \quad (6)$$

In the dissipative region, the exponents $\xi^L(q)$ have the trivial scaling $\xi^L(q) = q/2$. However, in the inertial range, one observes a clear scaling with a different exponent that varies non-linearly with the order of the structure function—the values of the relative scaling exponents for three different turbulent Reynolds numbers are reported in Table II. If one expands the resulting intermittency spectrum to quadratic order, one obtains a very good fit for the above data for the range of investigated values of R_λ , with a quadratic expansion:

$$\xi^L(q) = (1/2 + \lambda_L^2) q - \lambda_L^2 q^2/2 \quad \text{with} \quad \lambda_L^2 = 0.115 \pm 0.01. \quad (7)$$

(We emphasize that we do not assume a lognormal model for $\xi^L(q)$, but simply that a higher order expansion of the intermittency spectrum would be meaningless with the statistics reported here). The value of the Lagrangian intermittency parameter λ_L^2 is significantly larger than the one generally observed in the Eulerian statistics. Indeed, experimental and numerical observations⁽²⁶⁾ in Eulerian coordinates are well represented by the following quadratic spectrum:

$$\xi^E(q) = (1/3 + \lambda_E^2) q - \lambda_E^2 q^2/3 \quad \text{with} \quad \lambda_E^2 = 0.025. \quad (8)$$

The fact that intermittency may be more pronounced in Lagrangian coordinates has been originally remarked by Borgas.⁽²⁷⁾ We give hereafter a similar argument to relate Eulerian and Lagrangian statistics, after a

Table II. Value of the Lagrangian Relative Structure Function Exponents, for Three Different Turbulent Reynolds Numbers (R_λ , Based on the Taylor Microscale)

R_λ	310	740	1100	error
ξ_1	0.56	0.56	0.56	± 0.01
ξ_2	1	1	1	
ξ_3	1.32	1.33	1.34	± 0.02
ξ_4	1.54	1.56	1.58	± 0.06
ξ_5	1.68	1.73	1.76	± 0.1
ξ_6	1.8	1.8	1.9	± 0.1

remark by B. Castaing.⁽²⁸⁾ It relies on the Kolmogorov–Obukhov 1962 idea^(29,30) that intermittency is related to the non-uniformity of energy transfer. In Eulerian coordinates one writes:

$$D_q^E(\ell) \propto \langle \epsilon_\ell^{q/3} \rangle \ell^{q/3} \propto \ell^{\alpha^E(q/3)} \ell^{q/3}, \quad (9)$$

so that the Eulerian velocity intermittency exponents $\zeta^E(q)$ are related to the energy transfer exponents through:

$$\zeta^E(q) = \alpha^E(q/3) + q/3. \quad (10)$$

Similarly one writes in Lagrangian coordinates:

$$D_q^L(\tau) \propto \langle \epsilon_\tau^{q/2} \rangle \ell^{q/2} \propto \tau^{\alpha^L(q/2)} \tau^{q/2}, \quad (11)$$

so that

$$\zeta^L(q) = \alpha^L(q/2) + q/2. \quad (12)$$

The two statistics are related when the coarse-grained energy transfer ϵ_τ is interpreted in the framework of a Richardson cascade: a statistical time increment of duration τ corresponds to eddies size ℓ , such that $\ell^2 \propto \tau^3$. On then has:

$$\alpha^L(q) = \frac{3}{2} \alpha^E(q). \quad (13)$$

The intermittency coefficient λ^2 can then be estimated from the scaling of the flatness function. This yields:

$$\lambda_E^2 = -\frac{\partial \log(\langle \Delta_\ell u^4 \rangle / \langle \Delta_\ell u^2 \rangle^2)}{\partial \log \ell} = 2\alpha^E(2/3) - \alpha^E(4/3), \quad (14)$$

$$\lambda_L^2 = -\frac{\partial \log(\langle \Delta_\tau v^4 \rangle / \langle \Delta_\tau v^2 \rangle^2)}{\partial \log \tau} = 2\alpha^L(1) - \alpha^L(2), \quad (15)$$

so that:

$$\frac{\lambda_L^2}{\lambda_E^2} = \frac{2\alpha^L(1) - \alpha^L(2)}{2\alpha^E(2/3) - \alpha^E(4/3)} = \frac{3\alpha^E(1) - 3\alpha^E(2)/2}{2\alpha^E(2/3) - \alpha^E(4/3)} = \left(\frac{3}{2}\right)^3. \quad (16)$$

Using pure Kolmogorov–Richardson arguments, one finds that the intermittency coefficient should be at least 3.4 times larger in the Lagrangian domain than the Eulerian one.

5. INTERMITTENCY AND DYNAMICS

5.1. Experimental Observations

Intermittency is thus observed and quantified in both Lagrangian and Eulerian frameworks. In contrast to traditional Eulerian studies where intermittency is described in terms of multiplicative processes, we look here for a dynamical origin. We consider the statistics of the fluid particles fluctuating velocity in analogy with a random walk. We write a velocity increment over a time lag τ as the sum of contributions over very short time increments τ_1 :

$$\Delta_\tau v(t) = v(t+\tau) - v(t) = \sum_{n=1}^{\tau/\tau_1} \Delta_{\tau_1} v(t+n\tau_1). \quad (17)$$

If the incremental “steps” of duration τ_1 were independent (and identically distributed), the PDF $\Pi_\tau(\Delta v)$ would readily be obtained as a convolution of the elementary distribution at scale τ_1 , $\Pi_{\tau_1}(\Delta v)$ —plus an eventual convolution kernel to account for stationarity at large scales. Such a regular convolution process corresponds to the Kolmogorov K41 picture of turbulence;⁽¹⁾ the particle velocity fluctuations are Brownian and the scaling is monofractal.

Therefore if a multifractal behavior is to be observed, one should either have non-integrable acceleration fluctuations or the presence of long-range correlations in the dynamics, or both. The measurements of Bodenschatz’ group^(13,23) regarding the Lagrangian accelerations have shown that the former possibility must be ruled out, so that correlations must exist in the Lagrangian dynamics. To demonstrate it, we plot in Fig. 6 the time correlation of the elementary velocity increments; normalized correlation coefficients $\chi(f, g)(\Delta t) = \langle (f(t+\Delta t) - \langle f \rangle)(g(t) - \langle g \rangle) \rangle / \sigma_f \sigma_g$ are being computed both for signed velocity increments ($f, g(t) = \Delta_{\tau_1} v(t)$) and for their amplitude ($f, g(t) = |\Delta_{\tau_1} v(t)|$). First, one observes that the auto-correlation of the signed increments, $\Delta_{\tau_1} v(t)$, decays very rapidly: the correlation coefficient drops under 0.05 for time separations larger than $5\tau_1$. However, if one considers the amplitude (i.e., the modulus) of the “steps” ($|\Delta_{\tau_1} v(t)|$), one finds that the auto-correlation decays very slowly and only vanishes at the largest time scales of the turbulent motion. Recast in terms of the random walk, our results show that the amplitudes of the “steps” are long-range correlated in time although their directions are not. As this point is fundamental for our approach, we have verified it using a Lagrangian tracking algorithm in a Direct Numerical Simulation (DNS) of the Navier–Stokes equations, using a pseudo-spectral solver, at $R_\ell = 75$, and for the same ratio τ_1/T_L —see inset of Fig. 6. The results are in

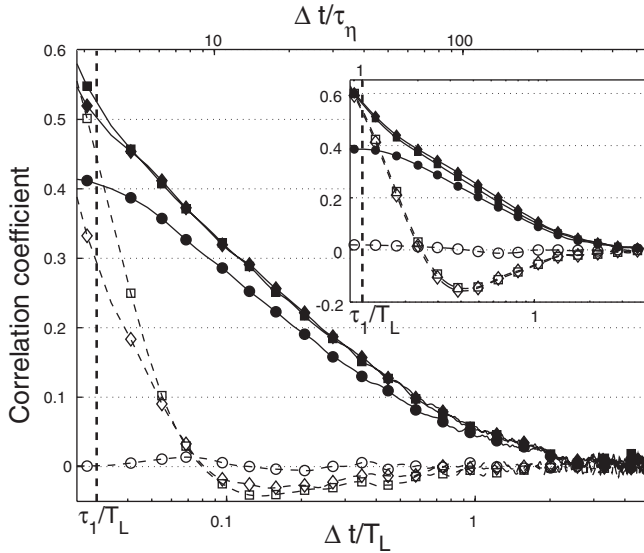


Fig. 6. Variation of the normalized correlation coefficient $\chi(f, g)(\Delta t) = \langle (f(t + \Delta t) - \langle f \rangle) \times (g(t) - \langle g \rangle) \rangle / \sigma_f \sigma_g$. Two velocity components are considered: the squares and diamonds mark the $\chi(\Delta_{\tau_1} v_x, \Delta_{\tau_1} v_x)$ and $\chi(\Delta_{\tau_1} v_y, \Delta_{\tau_1} v_y)$ auto-correlation functions while the circles mark the cross-correlation $\chi(\Delta_{\tau_1} v_x, \Delta_{\tau_1} v_y)$; curves with filled symbols are computed using the absolute value of the increments while the curves with open symbols are computed using the full signed increments. The main curve corresponds to the experiment at $Re = 740$, with $\tau_1 = 0.03T_L$. The inset shows similar results for a Direct Numerical Simulation at $Re = 75$.

remarkable agreement with our measurements. All increments are correlated for $\Delta t < \tau_1$, the time over which they are computed. Above τ_1 , the correlation of the signed increments rapidly drops while the correlation coefficient of their absolute values decays very slowly, to vanish only for $\Delta t > 3T_L$. This behavior is observed for τ_1 chosen from the smallest resolved time scales to inertial range values.

In order to proceed further, one needs to determine the functional form of these long range correlations of the magnitude of Lagrangian velocity increments. It turns out that a linear behavior is observed if one plots the variation of the connected magnitude of the increments as a function of their logarithmic separation in time:

$$\chi_{LM}(\Delta t) = \frac{\langle (\log |\Delta_{\tau_1} v_x|(t) - \langle \log |\Delta_{\tau_1} v_x| \rangle) (\log |\Delta_{\tau_1} v_x|(t + \Delta t) - \langle \log |\Delta_{\tau_1} v_x| \rangle) \rangle}{\langle (\log |\Delta_{\tau_1} v_x|(t) - \langle \log |\Delta_{\tau_1} v_x| \rangle)^2 \rangle}$$

$$\propto -\log \left(\frac{\Delta t}{T_L} \right). \quad (18)$$

The proportionality coefficient, as we will show in the next section, is the intermittency parameter λ^2 , as defined in Eq. (7).

5.2. A Multifractal Random Walk Model

Our observations of long time-correlations in the magnitude of elementary velocity increments also persist in the limit of very small time increments, and thus presumably for the acceleration of the fluid particle and thus for the forces acting on it. Theoretically, one would like to understand this behavior from the hydrodynamic forces in the Navier–Stokes equations. Such a direct analytical treatment is out of reach at present. However, in the Eulerian framework, work on the Kraichnan model⁽³⁾ has shown that intermittency can be traced back to model equations. For the Lagrangian problem considered here, we develop a similar approach and, as a first step, we propose a model dynamical equation of the Langevin type to describe the velocity fluctuations of a fluid particle. Stochastic modelling of Lagrangian velocity fluctuation has indeed long been used in turbulence.⁽¹⁸⁾ It is justified because one aims at understanding the statistical properties of the Lagrangian motion of fluid particles. In addition, the Langevin approach has long proven an invaluable tool of statistical mechanics.

In this procedure, one considers a one-dimensional variable, $W(t)$, representing the particle velocity, driven by a stochastic force. If this force is chosen as a white noise then $W(t)$ has the dynamics of Brownian motion: its statistics is monofractal with a similarity exponent equal to 1/2—the increments scale as $\langle |W(t+\tau) - W(t)|^p \rangle_t \sim \tau^{p/2}$, corresponding to the non-intermittent Kolmogorov 1941 picture. In order to account for intermittency, one needs to ascribe other properties to the stochastic force. Guided by our experimental results, we build a stochastic force having a random direction and a long-range correlation in its magnitude. Specifically, its direction is modeled by a Gaussian variable $G(t)$, chosen white in time, with zero mean and unit variance. The amplitude of the force, $A(t)$, being a positive variable, is written $A(t) = \exp[\omega(t)]$ where the magnitude $\omega(t)$ is a stochastic process that satisfies:

$$\langle \omega(t) \omega(t + \Delta t) \rangle_t = -\lambda^2 \ln(\Delta t / T_L) \quad \text{for } \Delta t < T_L, \quad (19)$$

and 0 otherwise— λ^2 being an adjustable parameter. When discretized, this dynamics corresponds to a one-dimensional Multifractal Random Walk (MRW).⁽³¹⁾ Analytical calculations show that the resulting dynamical variable $W(t)$ has multi-scaling properties. The moments have scaling laws,

$\langle |\Delta_\tau W|^q \rangle \sim \tau^{\zeta(q)}$, with $\zeta(q) = (1/2 + \lambda^2)q - \lambda^2 q^2/2$, so that λ^2 in Eq. (19) is the intermittency parameter of the model.⁽³¹⁾ It is a fundamental point that the same parameter λ^2 governs both the evolution of the PDFs of the increments (one-time statistics) and the time correlation of the process (two-time statistics).

We show that this model captures the essential features of the Lagrangian data. First, in order to test the relevance of Eq. (19), we have computed, from experimental and numerical data, the auto-correlation function of the logarithm of the amplitude of infinitesimal Lagrangian velocity increments, $\chi_{LM}(\Delta t)$. As shown by the line with filled circles in Fig. 7, the agreement between the model and the observations is excellent. It yields an estimate of the intermittency parameter $\lambda^2 = 0.115 \pm 0.01$.

In order to show the relevance of the model for the description of the one-time statistics of the Lagrangian increments $\Delta_\tau v$, we first note—Fig. 4, upper curve—that the choice $\lambda^2 = 0.115$ yields a PDF for the stochastic force that is in remarkable agreement with experimental measurements of fluid particle accelerations. Indeed in Fig. 4, the crosses are derived from the force in the MRW model whereas the continuous curve corresponds to the measurement of La Porta *et al.*⁽²³⁾ in a similar flow at a comparable Reynolds number. The agreement at larger time scales is evidenced on the

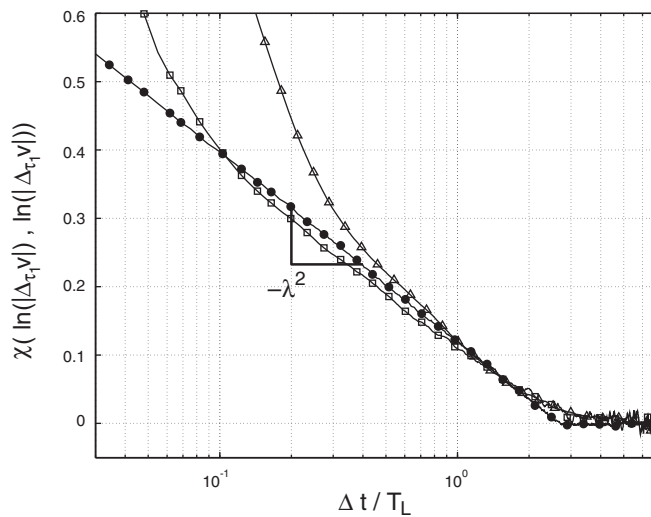


Fig. 7. Correlation in time of the magnitude of one component of the velocity increments, $\chi_{LM}(\Delta t)$, computed as in Eq. (18), for a time lag $\tau_1 = 0.03T_L$. Squares, experimental measurement; triangles, numerical simulation; and circles (filled), MRW model developed below.

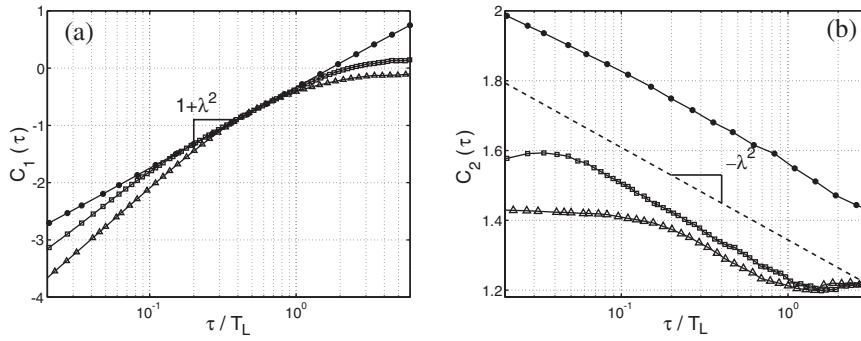


Fig. 8. Experimental (open squares) and numerical data (open triangles) compared to the predictions of the MRW model (filled circles). (a) and (b): first and second order cumulants, respectively, versus time scale τ .

behavior of the first two cumulants. Cumulants are computed with more reliability than the moments and are related to them through:

$$\langle |A_t v|^q \rangle = \langle \exp(q \ln |A_t v|) \rangle = \exp \left(\sum_n C_n(\tau) q^n / n! \right). \quad (20)$$

In the MRW model, one can analytically derive:⁽³¹⁾

$$C_1(\tau) = (1 + \lambda^2) \ln(\tau), \quad C_2(\tau) = -\lambda^2 \ln(\tau), \quad (21)$$

all higher order cumulants being null (the MRW model is thus an effective log-normal model of turbulence⁽²⁵⁾). The cumulants $C_1(\tau)$ and $C_2(\tau)$ computed from the experimental and numerical data are shown in Fig. 8 and compared to MRW model predictions when the intermittency parameter is set to the value $\lambda^2 = 0.115$ which is derived from the correlations in the dynamics (Fig. 6). One observes that in each case the agreement is excellent; the slope of the variation $\partial C_{1,2}(\tau) / \partial \ln \tau$ in the inertial range is correctly given by Eq. (21). The same intermittency parameter thus governs the anomalous scaling of the Lagrangian velocity increments and their long-time dynamical correlations.

6. CONCLUDING REMARKS

Long-time correlations in the Lagrangian dynamics are found to be a key feature for the understanding of intermittency, which leads to a new dynamical picture of turbulence. Long-time correlations and the occurrence of very large fluctuations at small-scales dominate the motion of a fluid particle. It can be understood if, along its trajectory, the particle encounters

very intense small-scale structures (vortices and stagnation points) over a more quiet background. Intermittency is then due to the nature and distribution of these small scale structures. Indeed, the analogy with a random walk suggests that the statistics at all scales can be recovered if one ascribes two properties to the small scales: (1) the probability density function of fluid particle accelerations, and (2) the functional form of their time correlations. In the Lagrangian framework, these features are directly linked to the Navier–Stokes equations that govern the elementary changes in the velocity (momentum) of the fluid particles. It thus gives a possibility to derive intermittency from the constitutive physical equations. Although this may be quite a theoretical challenge, direct numerical simulations look promising as they allow the study of the flow dynamical fields (pressure, velocity gradient tensor, etc.) along the trajectory of individual fluid particles.

ACKNOWLEDGMENTS

This work is supported by the French Ministère de La Recherche (ACI No. 226), and the Centre National de la Recherche Scientifique under GDR Turbulence. Numerical simulations are performed at CINES (France) using an IBM SP computer. We thank B. Castaing, P. Chanais, P. Holdsworth, B. Portelli, for fruitful discussions and we gratefully acknowledge the help of P. Metz, M. Moulin, and L. de Lastelle.

REFERENCES

1. U. Frisch, *Turbulence* (Cambridge University Press, Cambridge, 1995).
2. A. Pumir, B. Shraiman, and M. Chertkov, *Phys. Rev. Lett.* **85**:5324 (2001).
3. G. Falkovich, K. Gawedzki, and M. Vergassola, *Rev. Modern Phys.* **73**:913 (2001).
4. N. Mordant, O. Michel, and J.-F. Pinton, *J. Acoust. Soc. Am.* **112**:108–119 (2002).
5. S. Douady, Y. Couder, and M.-E. Brachet, *Phys. Rev. Lett.* **67**:983–986 (1991).
6. J.-F. Pinton and R. Labbé, *J. Phys. II France* **4**:1461–1468 (1994).
7. J. Maurer, P. Tabeling, and G. Zocchi, *Europhys. Lett.* **26**:31 (1994).
8. N. Mordant, J.-F. Pinton, and F. Chill, *J. Phys. II France* **7**:1729–1742 (1997).
9. N. Mordant and J.-F. Pinton, *Eur. Phys. J.* **B18**:343–352 (2000).
10. N. Mordant, *Mesure Lagrangienne en turbulence*, Ph.D. thesis, École Normale Supérieure de Lyon (2001).
11. O. Michel and H. Clergeot, Multiple source tracking using a high resolution method, *ICASSP'91*, Toronto, Canada (1991), pp. 1277–1280.
12. L. L. Scharf, *Statistical Signal Processing; Detection, Estimation, and Time Series Analysis* (Addison–Wesley, 1991).
13. G. A. Voth, K. Sathyanarayan, and E. Bodenschatz, *Phys. Fluids* **10**:2268 (1998).
14. P. K. Yeung and S. B. Pope, *J. Fluid Mech.* **207**:531 (1989).
15. Y. Sato and K. Yamamoto, *J. Fluid Mech.* **175**:183 (1987).
16. M. Virant and T. Dracos, *Meas. Sci. Technol.* **8**:1539 (1997).

17. S. B. Pope, *Annu. Rev. Fluid Mech.* **26**:23 (1994).
18. B. L. Sawford, *Phys. Fluids A* **3**:1577 (1991).
19. R-C. Lien, E. A. D'Asaro, and G. T. Dairiki, *J. Fluid. Mech.* **362**:177 (1998).
20. P. K. Yeung, *J. Fluid Mech.* **427**:241 (2001).
21. S. R. Hanna, *J. Appl. Meteorol.* **20**:242 (1981).
22. S. Du, B. L. Sawford, J. D. Wilson, and D. J. Wilson, *Phys. Fluids* **7**:3083 (1995).
23. A. La Porta, G. A. Voth, A. Crawford, J. Alexander, and E. Bodenschatz, *Nature* **409**:1017 (2001).
24. R. Benzi, S. Ciliberto, C. Baudet, G. Ruiz Chavarria, and R. Tripiccone, *Europhys. Lett.* **24**(4):275–279 (1993).
25. J. Delour, J.-F. Muzy, and A. Arnéodo, *Eur. Phys. J. B* **23**:243 (2001).
26. A. Arnéodo *et al.*, *Europhys. Lett.* **34**:411 (1996).
27. M. S. Borgas, *Philos. Trans. Roy. Soc. London Ser. A* **342**:379 (1993).
28. B. Castaing, private communication.
29. A. N. Komogorov, *J. Fluid Mech.* **13**:82 (1962).
30. A. M. Obhukov, *J. Fluid Mech.* **13**:77 (1962).
31. E. Bacry, J. Delour, and J.-F. Muzy, *Phys. Rev. E* **64**:026103 (2001).